Role of solvent in enhancing the production of butyl levulinate from fructose

Daniele Di Menno Di Bucchianico, Jean-Christophe Buvat, Mélanie Mignot,
Valeria Casson Moreno, Sébastien Leveneur

1   Role of solvent the production of butyl levulinate from fructose

2   Daniele Di Menno Di Bucchianico[1,2], Jean-Christophe Buvat[1], Mélanie Mignot[3], Valeria Casson

3   Moreno[2] and Sébastien Leveneur[1,*]

4   [1]Normandie Univ, INSA Rouen, UNIROUEN, LSPC, EA4704, 76000 Rouen, France ;

5   [2]Dipartimento di Ingegneria Chimica, Civile, Ambientale e dei Materiali, Alma Mater Studiorum—

6   Università di Bologna, via Terracini 28, 40131 Bologna, Italy;

7   [3]COBRA UMR CNRS 6014, Normandie Université, INSA de Rouen, avenue de l'Université, Saint-

8   Etienne-du-Rouvray, 76800, France

9   *corresponding author: sebastien.leveneur@insa-rouen.fr

10   **Abstract:** The use of alkyl levulinates is growing interest in fuels. Adding n-butyl levulinate (BL) to fuels

11   presents some benefits compared to ethyl levulinate. The conventional production route of BL is from

12   the esterification of levulinic acid, but the latter compound presents some corrosion issues. Alcoholysis

13   of fructose by butanol over cation exchange resins (solid catalyst) seems to be a better alternative. The

14   effect of water addition, solvent, swelling effect (from the cation exchange resin), and fructose solubility

15   at temperatures higher than 25°C are unclear on this reaction. To understand these effects, the

16   alcoholysis of fructose by butanol at 110°C in different solvents, e.g., gamma-valerolactone (GVL), were

17   studied in a pressurized autoclave in an inert environment. The dissolution study was conducted in a

18   temperature range of 20-120°C in different solvents. The concentration profiles of fructose, 5-

19   (hydroxymethyl)furfural (HMF), 5-(butoxymethyl)furfural (BMF) and BL were analyzed in different

20   solvents: butanol/water, butanol, butanol/GVL/water and butanol/GVL. We found that using a

21   butanol/GVL (70/30 wt%) solvent is better from the conversion and dissolution viewpoints.

22   **Keywords:** Mass transfer; Alcoholysis; Solvent effect; Solid catalyst

23

1. Introduction

The depletion of fossil fuels together with growing concern about the environmental impact of human activities is pushing the research for new and renewable sources of energy and raw materials. Lignocellulosic biomass (LCB) is considered a valuable ally in producing chemicals, fuels, and materials, being an abundant, renewable and carbon-fixing resource. In opposition to food biomass which can incur in the food versus fuel dilemma, LCB (second generation biomass) represents an excellent alternative feedstock in biorefinery [1,2]. In this context, the use of lignocellulosic biomass and its conversion to value-added chemicals and fuels has become increasingly widespread. [3,4]. Considering LCB main components: lignin, cellulose and hemicellulose, the development of lignin valorization into chemicals is still under progress due to its complex and heterogeneous aromatic polymeric structure [5–11]. Meanwhile, the industrial valorization of cellulose and hemicellulose into so-called platform molecules is mature [12–18]. Several pretreatments allow fractioning these complex biomass polymers into simple sugar-monomers, valuable through different chemical pathways to several platform molecules such as 5-(Hydroxymethyl)furfural (HMF), glycols, sorbitol or levulinic acid and alkyl levulinates (Fig. 1) [17–19].
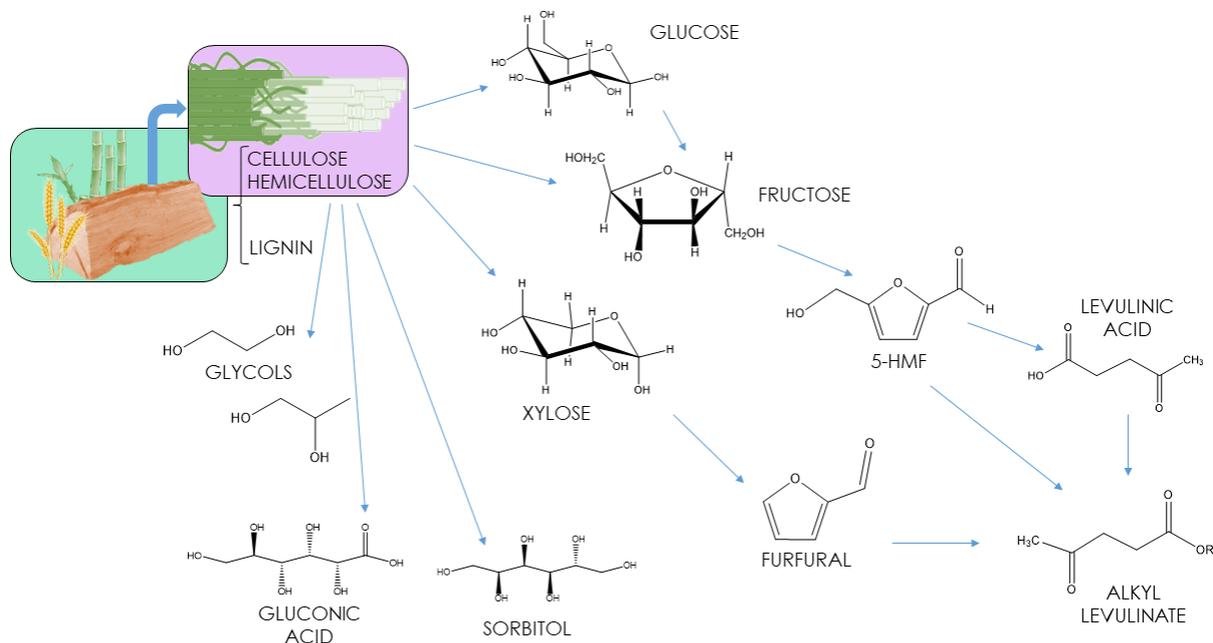

Fig. 1. Valorization of cellulose adapted from literature [18].

42 Alkyl levulinates are promising and versatile platform molecules issued from cellulose and/or

43 hemicellulose alcoholysis with broad industrial applications. Esters of levulinic acid can simply be

44 produced by esterification of levulinic acid [20–23], but the low yield in the production of levulinic acid,

45 together with the high costs of separation and purification, make this route less beneficial compared to

46 using more affordable starting feedstocks as biomass-derived monosaccharides: glucose and fructose

47 [4,24–31]. Although glucose is the most abundant monomers and the least expensive substrate over

48 other monomers [32], fructose shows higher molecular instability and faster reactivity to be dehydrated

49 to 5-(hydroxymethyl)furfural, first intermediate in the pathway to alkyl levulinate, whereas glucose must

50 first be isomerized to fructose [33].

51 From an energy viewpoint, alkyl levulinates can be used as blending components for biodiesel or fuel

52 oxygenate additives [34,35], improving fuel quality and reducing pollutant emission [36,37]. In 2017,

53 Tian et al. demonstrated that methyl and ethyl levulinate have higher anti-knock quality than Euro95

54 gasoline [38]. Wang et al. investigated the use of ethyl levulinate as a diesel blend, resulting in a higher

55 closed cup flash point, oxygen content, and lower kinematic viscosity compared to n-butanol [39].

56 Christensen et al., have shown that butyl levulinate (BL) can improve conductivity, cold flow properties

57 and lubricity of diesel fuel and reduce its vapor pressure [40]. Furthermore, BL was found to remain in

58 solution with diesel down to the fuel cloud point and to have more compatibility with elastomers,

59 compared to ethyl levulinate, which tends to separate from diesel at a temperature below 0 °C and

60 results to be more corrosive [40]. Frigo et al. showed that diesel fuel blended with a mixture of butyl

61 levulinate and dibutyl ether could reduce particulate emissions without changing engine power efficiency

62 or increasing the NOx emission [41].

63 Alcoholysis of sugar monomers to BL is catalyzed mainly by Brønsted-acids [42]. Traditional mineral

64 acids are gradually being substituted by heterogeneous acid catalysts, cause of equipment corrosion,

65 separation and neutralization costs. Zeolites, ion exchange resins, metal oxides, nanomaterials and

66 other numerous solid catalysts have been tested to produce butyl levulinate from biomass-derived

67 carbohydrates [42].

68 An et al. studied the production of BL from the alcoholysis of different carbohydrates and found that

69 ferric sulfate was the most efficient [33]. They found that with a catalyst loading of 5 g/L, a reaction

70 temperature of 190°C, and a fructose concentration of 25 g/L, the yield of BL was found to be 62.8 mol%

71 for 3 hours of reaction time.

72   Higher alkyl levulinate yields from fructose were also confirmed by Liu et al. [29] using sulfonic acid-

73   functionalized carbon materials. BL has been produced with a yield of 78 mol% after 12 h and complete

74   fructose conversion [29].

75   Ramirez et al. made an in-depth assessment on the use of ion-exchange resins for the direct

76   transformation of fructose into BL by alcoholysis [43]. Using a water/butanol mixture, they detected BL

77   production only at a temperature higher than 100°C. They also showed that between 17-37% of fructose

78   is lost in humins production. They studied catalyst reuse and found that fresh and twice-reused catalysts

79   have similar activity. In this assessment, gel-type Dowex 50Wx2 resulted in the best catalyst according

80   to BL yield.

81   Several research studies on the alcoholysis of sugars into alkyl levulinate essentially focus on the

82   catalysis. To the best of our knowledge, there are not many studies on the crucial role of solvent, which

83   can affect the reaction kinetics and the product selectivity, sugar dissolution, polymerization, and

84   degradation. Sun et al. reported that the conversion of sugars and furans, particularly fructose and 5-

85   (hydroxymethyl)furfural, is different in different solvents, depending on their polarity and protic aprotic

86   nature [44]. Protons transfer is a key point in the acid-catalyzed alcoholysis mechanism, and the solvent

87   plays a crucial role [45]. Sugar monomers showed high reactivity in water, one of the most used solvents

88   in lignocellulosic biomass derivatives pretreatment and conversion. Water provides a good solvation

89   environment, allowing high dissociation of Brønsted acids and also high solubility of carbohydrates [46].

90   On the other hand, the high reactivity in aqueous systems results in greater instability of sugars and

91   furan intermediates which tend to undergo acid-catalyzed side reactions, as production of by-product

92   humins [44,47,48]. An alternative to minimize side reactions is using polar organic solvents, particularly

93   alcohols [47,48]. Some studies reported promising alkyl levulinates yields from fructose alcoholysis in

94   pure alcohols. Ramirez et al. [43] obtained a 73.4 mol% butyl levulinate yield from fructose alcoholysis

95   in pure butanol, and Sun et al. [44] a yield of 51.6 mol% ethyl levulinate from fructose alcoholysis in pure

96   ethanol, both catalyzed by ion exchange resins. Excess of alcohol results in a major control of the

97   conversion steps, protons transfer and limitation of the polymerization of sugars and furans [44,46]. In

98   pure butanol solvent, the selectivity of BL can also be lowered by the side reaction of etherification

99   producing dibutyl ether [43,49,50]. Besides the polar protic alcoholic medium, some studies highlighted

100   the role of polar aprotic solvents in lowering unwanted degradation reactions of intermediates [51,52].

101   The introduction of co-solvents might further minimize possible side-reaction products. Among polar

102   aprotic solvents, γ-valerolactone (GVL) may be a valid co-solvent in fructose alcoholysis. Several

103   patents suggested it as a green alternative to classical hazardous solvents since it can be produced

104   starting from derived-biomass fructose via hydrogenation of levulinic acid or alkyl levulinates [53]. In

105   2014, M.A. Mellmer et al. [52] demonstrated the benefits of using polar aprotic solvents, such as GVL,

106   for acid-catalyzed reactions. Capecci et al. [54] reported the synthesis of GVL by hydrogenation of butyl

107   levulinate, identifying an excess of GVL as the best solvent system. Although the REACh registration is

108   still missing for GVL, some acute toxic data (LD_{50} oral-rat = 8800 mg/kg), its overall structure and

109   properties suggest its stability, biodegradability and not toxicity [55], responding to the principle of benign

110   solvents and auxiliaries of Green Chemistry principles [56].

111   Despite many publications on this topic, several aspects are missing in the literature concerning the

112   alcoholysis of fructose over cation exchange resins, such as the solvent effect, the role of water, the

113   resin swelling and fructose dissolution within a temperature range of 60-100°C. In this study, a deep

114   investigation on the production of BL from the fructose alcoholysis was carried out over an ion exchange

115   resin: Amberlite IR-120. Being very effective in sugar monomers conversion and esterification reactions

116   [57–60], Amberlite IR-120 was chosen because of its good stability, high proton capacity, affordability

117   and recyclability without a significant decrease in its activity [58,61,62]. Solvent effects on the production

118   of BL and intermediates were evaluated as well as on the fructose dissolution at different temperatures.

119   A mass transfer study was performed, and the swelling of Amberlite IR-120 was also measured

120

121   2. Experimental section

122   2.1 Chemicals

123   Fructose (≥ 99% purity), 5-(hydroxymethyl)furfural (HMF, 99% purity), 5-(ethoxymethyl)furfural (EMF,

124   97% purity) and γ-valerolactone (≥ 99% purity) were purchased from Sigma-Aldrich.

125   1-Butanol (BuOH, ≥ 99,5 % purity), butyl levulinate (BL, ≥ 98% purity), acetonitrile (ACN, ≥ 99,9% purity),

126   butyl formate (BF, ≥ 97% purity) and acetone (≥ 99,9% purity) from VWR chemicals. Amberlite IR120

127   (H$^+$ form, ion-exchange resin) commercial catalyst provided by Acros Organics. Nitrogen gas (N$_2$ purity

128   > 99,999 vol%) from Linde. All chemicals were employed without further purification.

129   2.2 Analytical methods

130   Reaction samples were analyzed by combining gas and liquid chromatography. HPLC Agilent 1100

131   Series was employed to quantify fructose, equipped with a SUPELCOSIL LC-NH2 column (250 mm x

132   4.6 mm x 5 µm), a UV detector set at 191 nm, and by using a mixture of acetonitrile and ultrapure water

133   (90:10 v/v %) as mobile phase, with a flow rate of 1 mL/min and constant column temperature of 30 °C.

134   Reaction products, such as HMF, BL, 5-(butoxymethyl)furfural (BMF), and solvent systems were

135   detected by Bruker Scion 456-GC, equipped with a VF-1701ms Agilent column (60.0 m x 250 µm x 0.25

136   µm) and a flame ionization detector (FID). The injector and detector temperature were 250 °C, and the

137   oven temperature was programmed from 40 °C to 250 °C with 20 °C/min of ramp rate. All experimental

138   quantifications were based on daily calibration curves with standard solutions of pure commercially

139   available chemicals. EMF was used as a reference for the BMF calibration curve due to its commercial

140   unavailability. Each experimental sample was analysed three times to estimate the error in the analytical

141   method, in term of standard deviation.

142   Fructose conversion, butyl levulinate yield and catalyst loading were defined as follows:

143    $$\text{Fructose conversion (\%)} = \left(1 - \frac{\text{mole of fructose after the reaction}}{\text{initial mole of fructose}}\right) * 100 \qquad (1)$$

144    $$\text{BL yield (\%)} = \frac{\text{mole of BL after the reaction}}{\text{initial mole of fructose}} * 100 \qquad (2)$$

145    $$\text{Catalyst loading } (\omega_{\text{CAT}}) = \frac{\text{mass of catalyst}}{\text{liquid volume}} \text{ (g/L)} \qquad (3)$$

146

147   2.3 Experimental set-up

148   The alcoholysis reaction runs were performed in a 300 mL Parr stainless steel batch reactor, under

149   isothermal and isobaric conditions. The reactor was equipped with an electrical heating jacket and a

150   cooling coil, together with a thermocouple capable of measuring the reaction temperature and

151   communicating with the temperature controller. The presence of a gas entrainment impeller (diameter

152   2.5 cm) with a hollow shaft provided a uniform mixing of the reacting mixture.

153   For each experiment, the reactor was loaded with 1.6 g of fructose, 35 g/L of catalyst loading (4.5 – 4.9

154   g of catalyst) and a fixed volume of liquid. After loading the reaction mixture, catalyst and assembling

155   the reactor, the system was pressurized with nitrogen at 20 bars to limit the gas-liquid partition of the

156   liquid phase [43,58]. Then, the temperature heater and rotation stirrer were switched on. The first sample

157   was collected when the desired temperature was reached (time zero). Following the time zero sample,

158   samples were collected at 5 min, 30 min, and then every hour up to 7 h. The reaction temperature was

159   fixed to 110 °C, demonstrated by preliminary experiments to be the optimum between catalytic activity

160   and catalyst resistance towards temperature. Indeed, sulfonic groups, i.e., active sites, from Amberlite

161   IR-120 can leach when the temperature is higher than 120°C. Table 1 shows the experimental matrix

162   with the different solvent systems.

163   Table 1: Experimental matrix with the initial amount of fructose, butanol, water and GVL.

	Run	Fructose (g)	Butanol wt%	Water wt%	GVL wt%	ω_{CAT} (g/L)	T(°C)	rpm	Reaction time (h)	Inert gas
No GVL	1	1.6	83	17	0	35	110	800	7	N_2 (20 bar)
	2	1.6	91.5	8.5	0	35	110	800	7	N_2 (20 bar)
	3	1.6	96	4	0	35	110	800	7	N_2 (20 bar)
	4	1.6	100	0	0	35	110	800	7	N_2 (20 bar)
GVL	5	1.6	2.5	8.5	89	35	110	800	7	N_2 (20 bar)
	6	1.6	60.5	8.5	30	35	110	800	7	N_2 (20 bar)
	7	1.6	76.5	8.5	15	35	110	800	7	N_2 (20 bar)
	8	1.6	70	0	30	35	110	800	7	N_2 (20 bar)

164

165   Amberlite IR-120 was pre-treated before its use, as described by Leveneur et al. [62]. The catalyst was

166   washed through several cycles in water and a final one in butanol, which is the main reaction solvent,

167   after being dried in an oven at 90 °C at atmospheric pressure for 5 hours. Amberlite IR-120 is a cation

168   exchange resins composed of sulfonated styrene-divinyl benzene (PS-DVB) matrix with sulfonic acid

169   functional groups. The catalyst is a gel-type resin, bead-shaped, in which PS-DVB copolymers result in

7

170   a set of tangled chains with no spaces between them in the dry state. The degree of cross-linking, linked

171   to the level of divinylbenzene, represents the tightness of the resin. Table 2 shows the properties of

172   Amberlite IR-120.

173   Table 2: Properties of Amberlite IR-120 according to the manufacturer (Acros Oganics).

Supplier	Acros Organics
Structure	Styrene-divinylbenzene
Resin type	Gel-type
Cross linking (DVB%)	8
Moisture content (% mass)	48-58
Capacity by dry weight (m_{eq}/g)	4.4
Native particle size range (µm)	≥ 94 % (300 < d < 1180 µm)

174

175   2.4 Mass transfer study

176   To evaluate the effect of internal mass transfer, it is important to measure the effect of different particle

177   size ranges on the kinetics. Thus, the dried catalyst particles were sieved. As a result, the dried particle

178   size distribution (PSD) evidenced a high percentage (ca. 84 %) of particles with diameters higher than

179   500 µm and the remaining particles with diameters between 300 and 500 µm. The influence of external

180   and internal mass transfer resistances was investigated by varying agitation speed and particle size. As

181   shown in Table 3, varying the rotating speed between 500 and 1000 rpm, the external mass transfer

182   limitation was studied for the finest particle size distribution (runs 1',2',3' in Table 3). An optimum rotating

183   speed was selected to supress the external mass transfer resistance. The presence of internal mass

184   limitation was examined by considering the different particle size distribution (finest, highest and native

185   distribution; Runs 4',5',6' in Table 3).

186   Table 3: Experimental matrix for external and internal mass transfer limitation investigations.

	RUN	PSD	Fructose (g)	Butanol wt%	Water wt%	ω_{CAT} (g/L)	T(°C)	rpm	t(h)	Inert gas
Ext.	1'	Fine	1.6	83	17	35	110	500	7	N_2 (20 bar)
	2'	Fine	1.6	83	17	35	110	800	7	N_2 (20 bar)
	3'	Fine	1.6	83	17	35	110	1000	7	N_2 (20 bar)
Int.	4'	Fine	1.6	83	17	35	110	800	7	N_2 (20 bar)
	5'	High	1.6	83	17	35	110	800	7	N_2 (20 bar)
	6'	Native	1.6	83	17	35	110	800	7	N_2 (20 bar)

187

188

189 Being characterized by cross-linked styrene-divinylbenzene, the particle size of Amberlite IR120 is also

190 affected by the swelling effect due to the solvent. In other words, even if the amount of dried catalyst is

191 the same, the kinetics could be different if the solvent is different due to different swelling behavior. The

192 same procedure described in the article of Russo et al. was used [58,63]. Based on the Bodamer and

193 Kunin procedure [64], the swelling degree was investigated in each solvent system to observe the

194 catalyst behavior in all solvents. The parameter was evaluated by adding an aliquot of 20 mL of dry

195 catalyst to a graduated cylinder of 100 mL. The initial volume was read to the nearest 0.5 mL. Then, the

196 resin was covered with the specific solvent mixture to fill the cylinder volume without shaking and

197 tapping. After 120 h, the volume was read, and the swelling percentage was calculated as follows:

198 $\%SW = \frac{\text{final volume } (V_{\text{final}}) - \text{initial volume } (V_{\text{initial}})}{\text{initial volume } (V_{\text{initial}})} * 100$ (4)

199

200 2.5 Fructose dissolution investigation

201 The fructose dissolution has been measured in the different solvent mixtures considered in this study.

202 By using the same experimental equipment described above, a modified analytical method was applied

203 [65]; a solvent mixture of 140 mL volume together with a known amount of fructose (i.e. the specific

204 fructose concentration of 11 g/L used in the alcoholysis experiments) is added to the system, kept in

205 agitation at 800 rpm, at constant temperature and pressure and for a period of time sufficient to

206 determine the equilibrium of the system. Engasser et al. [66] observed a rapid initial phase in the

207 dissolution kinetics of fructose in which around 40% of the maximal concentration was reached in less

208 than 5 minutes. Thus, a time interval of 30 min was assumed as sufficient to reach the equilibrium in

209 this study. The system was tested under different temperature conditions by measuring the fructose

210 concentration at each temperature (Fig. 2). In particular, fructose dissolution has been investigated in

211 pure butanol and butanol-GVL mixture 70/30 wt% (Table 4).
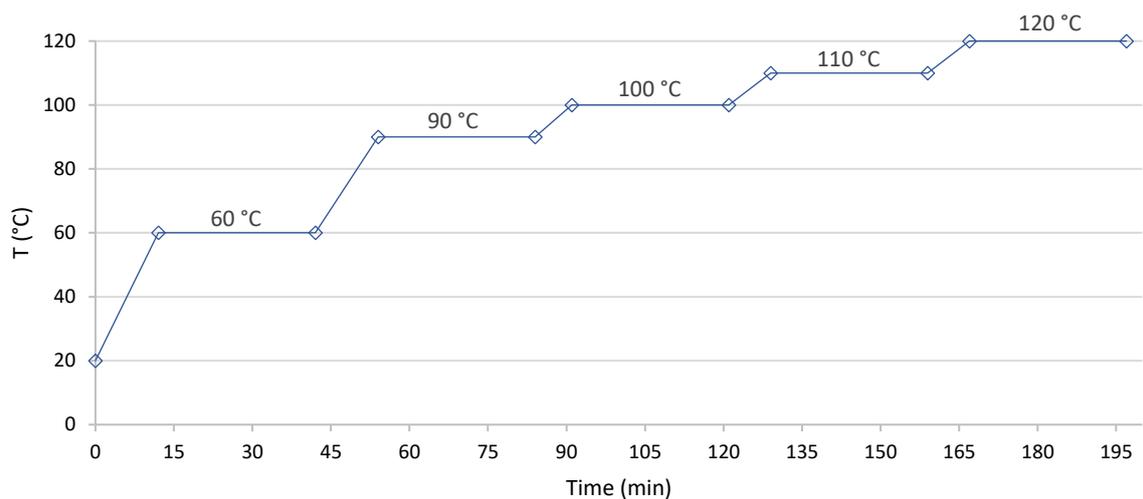
212

213   Fig. 2. Temperature profile versus time in fructose dissolution study.

214   Table 4: Experimental matrix for fructose dissolution study.

RUN	Fructose (g)	Butanol wt%	GVL wt%	rpm	Inert gas
S1	1.6	100	0	800	N_2 (20 bar)
S2	1.6	70	30	800	N_2 (20 bar)

215

216

217   3. Results and discussion

218   According to several articles, the reaction mechanism of fructose alcoholysis by butanol occurs

219   according to Fig. 3 [43,67–69]. In acidic system, fructose tends to be rapidly dehydrated to HMF, first

220   reaction intermediate. Through the alcoholic medium, HMF can be rehydrated to levulinic acid, then

221   esterified to butyl levulinate or be transformed into the corresponding ether, 5-BMF, then converted to

222   BL. Besides BL, butyl formate is also produced in an equimolar ratio. Experimentally, we observed the

223   pathway through 5-(butoxymethyl)furfural (HMF) as dominant since the production of levulinic acid is

224   very low, with concentrations close to zero throughout the reaction time. This might be due to the low

225   water concentration, which is insufficient to favor the rehydration of HMF rather than its etherification

226   with butanol [42]. For this reason, LA concentration trends were not considered in the subsequent

227   discussion of the results. Furthermore, the reaction scheme constituted of several consecutive and

228   parallel reactions also count the inevitable production of humins from polymerization side-reactions of

229   fructose and HMF. Studies claim that BMF does not degrade into humins [67].
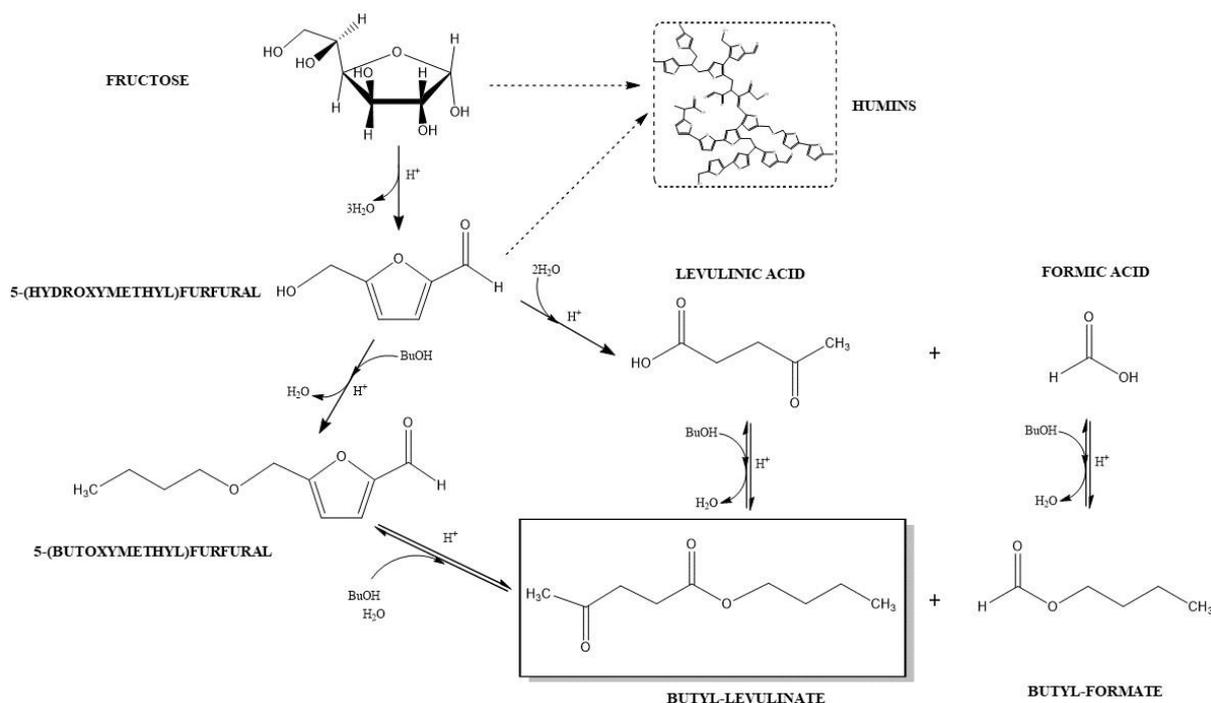

231   Fig. 3. Reaction steps for the fructose alcoholysis in an acid-catalyzed system.

237 3.1 Swelling effect

238 Table 5 shows that the swelling test of Amberlite IR120 showed similar behavior in the different solvents

239 and mixtures tested: pure butanol, pure GVL, pure water, BuOH/GVL/Water, BuOH/GVL and

240 BuOH/Water. Although slightly lower in pure GVL, the swelling factor is over 100 % in each solvent

241 system. Hence, the difference of kinetics for the alcoholysis of fructose by butanol over Amberlite IR-

242 120 in these solvents is not due to the swelling effect. Therefore, if the swelling effect is the same in

243 these solvents, the mass transfer study was only performed in BuOH/Water.

244 Table 5: Results from swelling study of Amberlite IR-120 at room temperature.

Solvent		V_0 (mL)	V_{fin} (mL)	%SW
Pure BuOH	-	20	42	110±5
Pure GVL	-	20	39	95±5
Pure Water	-	20	42	110±5
BuOH/GVL/Water	53/30/17 %wt	20	42	110±5
BuOH/GVL	70/30 %wt	20	42	110±5
BuOH/Water	83/17 %wt	20	41	105

245

246 While the results in pure water and binary mixture butanol-water are comparable with the ones obtained

247 in literature (around 100 % in water and 110 % in ethanol-water mixture) [58,64], the swelling effect in

248 pure butanol is higher than that reported in the literature for ethanol (40 % obtained by Bodamer and

249 Kunin [64], 70 % by Russo et al. [58]). The swelling parameter in the presence of GVL shows that the

250 addition of this solvent does not affect the swelling behavior of the catalyst.

251

252 3.2 Evaluation of external and internal mass transfer

253 -External mass transfer

254 Figs 4 show the effect of stirring rate on the kinetics of fructose alcoholysis. One can notice that the

255 fructose consumption is higher at 800 rpm than at 500 rpm or 1000 rpm (Fig. 4A). The fact that the

256 kinetics decreases from 1000 to 800 rpm is undoubtedly due to the vortex effect. Similar observation

257 can be done for BL, HMF and BMF concentration ratio (Fig. 4D, 4B, 4C). To decrease the effect of

258 external mass transfer resistance, experiments were performed at 800 rpm.
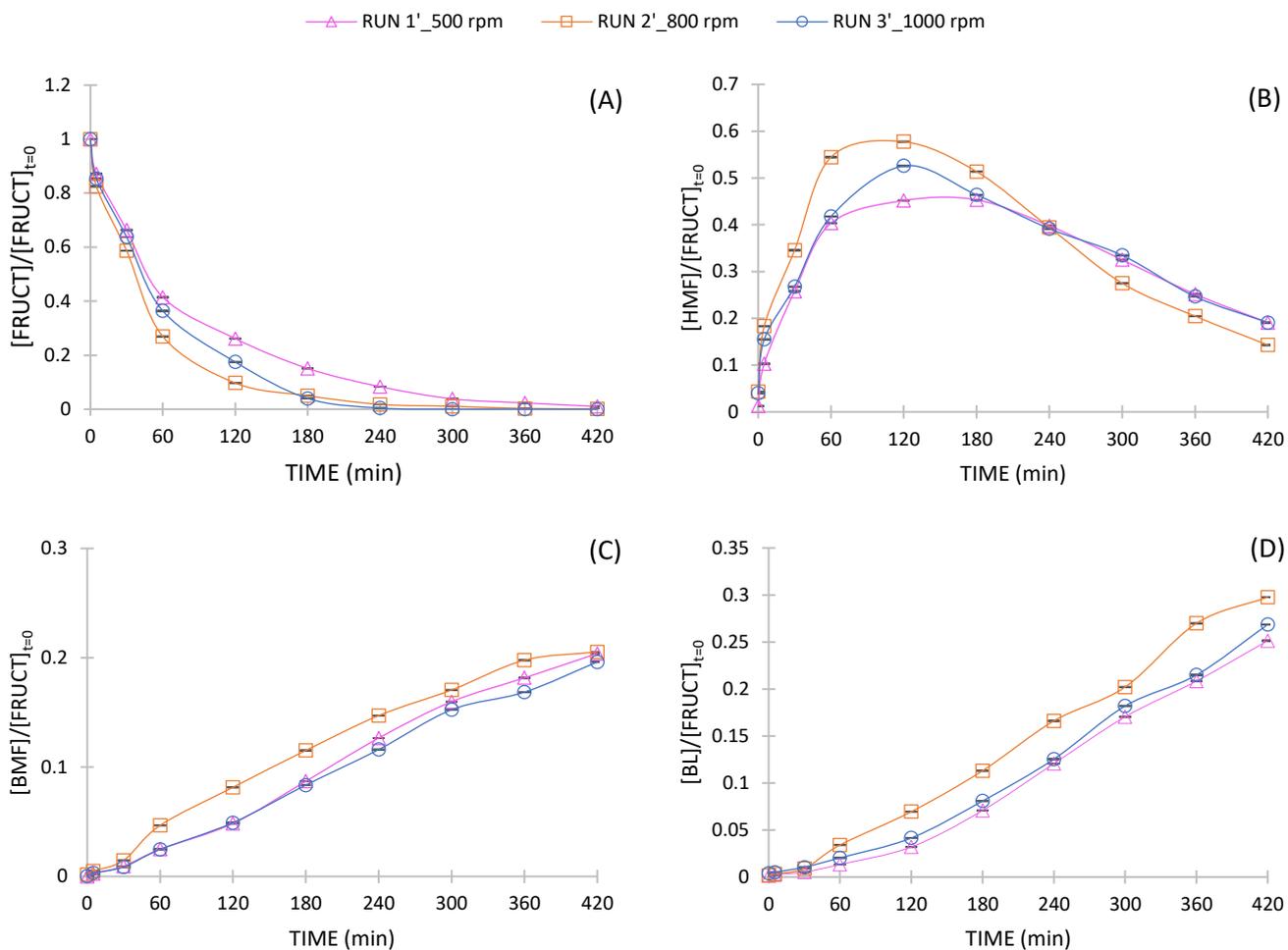
Fig. 4. Effect of the stirring rate on the concentrations (normalised with respect to the fructose concentration at time zero): (A) fructose, (B) HMF, (C) BMF, and (D) BL.

259

260

261

262   -Internal mass transfer

263   Figs 5 show the effect of catalyst PSD on the fructose alcoholysis. One can notice that in the operating

264   conditions of this study, the catalyst PSD of Amberlite IR120 has a very negligible effect on the trends

265   of fructose consumption (Fig. 5A), on HMF production (Fig. 5B), on BMF production (Fig. 5C), and on

266   BL production (Fig. 5D). Thus, the internal mass transfer resistance can be considered to be negligible.
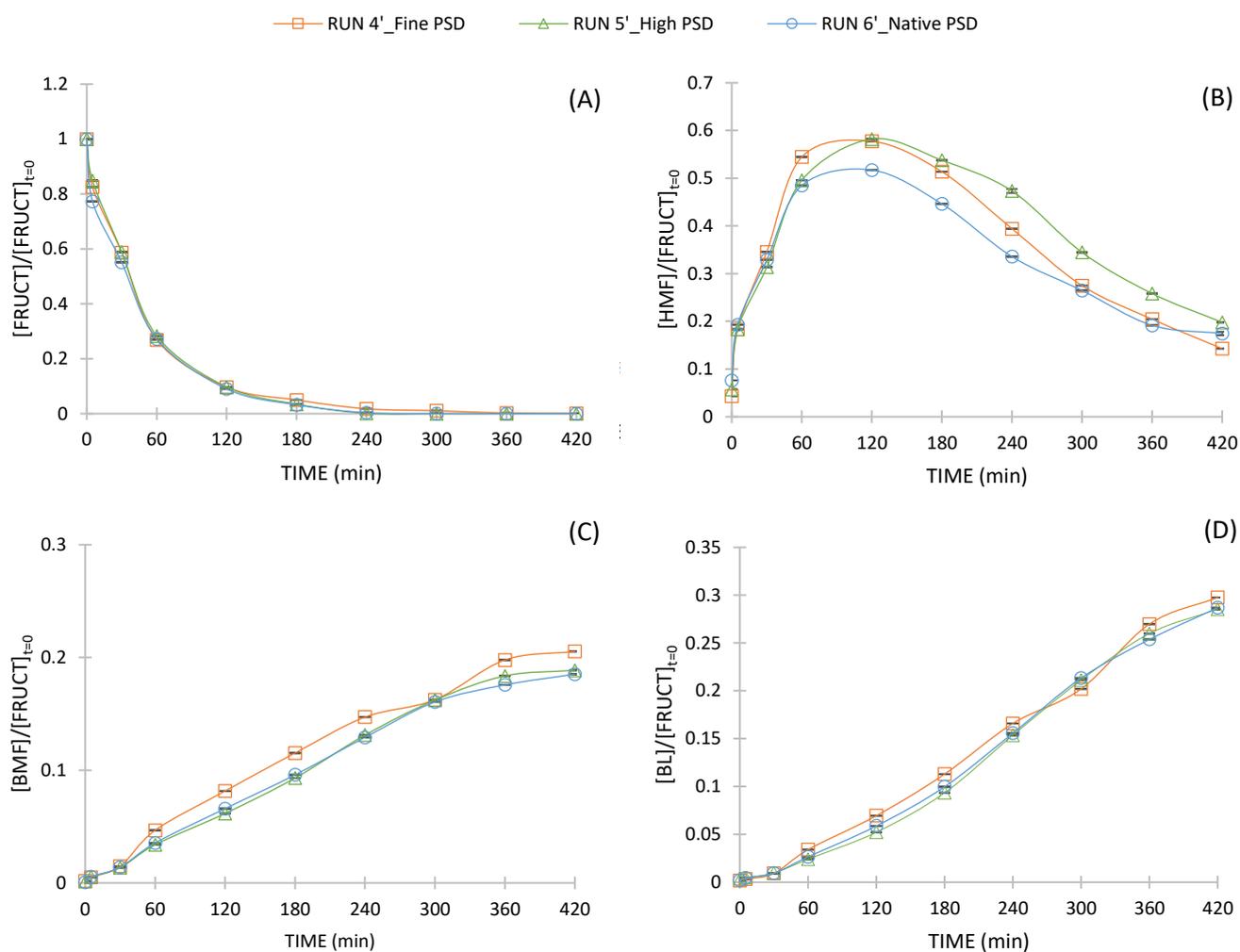
Fig. 5. Effect of catalyst PSD on the concentrations (normalised with respect to the fructose concentration at time zero): (A) fructose, (B) HMF, (C) BMF, and (D) BL.

267

268   Based on external and internal mass transfer study, the experiments were performed with native PSD

269   and at 800 rpm to avoid the interferences with mass transfer limitation.

270

271

14

272   3.3 Dissolution investigation

273   In the presence of water, even at low concentrations, it was observed that fructose dissolution could be

274   considered instantaneously. For that reason, the dissolution of fructose in a 70/30 wt% BuOH/GVL and

275   pure butanol solvent was studied.

276   The benefit of a 70/30 wt% BuOH/GVL compared to a pure butanol solution was found through fructose

277   dissolution. Fig. 6 shows that fructose solubility increases with temperature up to 110°C, fructose

278   degradation to humins is significant. Fructose dissolution results faster in a 70/30 wt% BuOH/GVL

279   solvent for temperature lower than 100°C, already reaching 33% of total concentration at 60°C and

280   complete dissolution at 100°C. The effect of BuOH/GVL solution in promoting fructose dissolution at

281   temperatures below 100 °C could be advantageous for catalysts suffering from thermal instability.
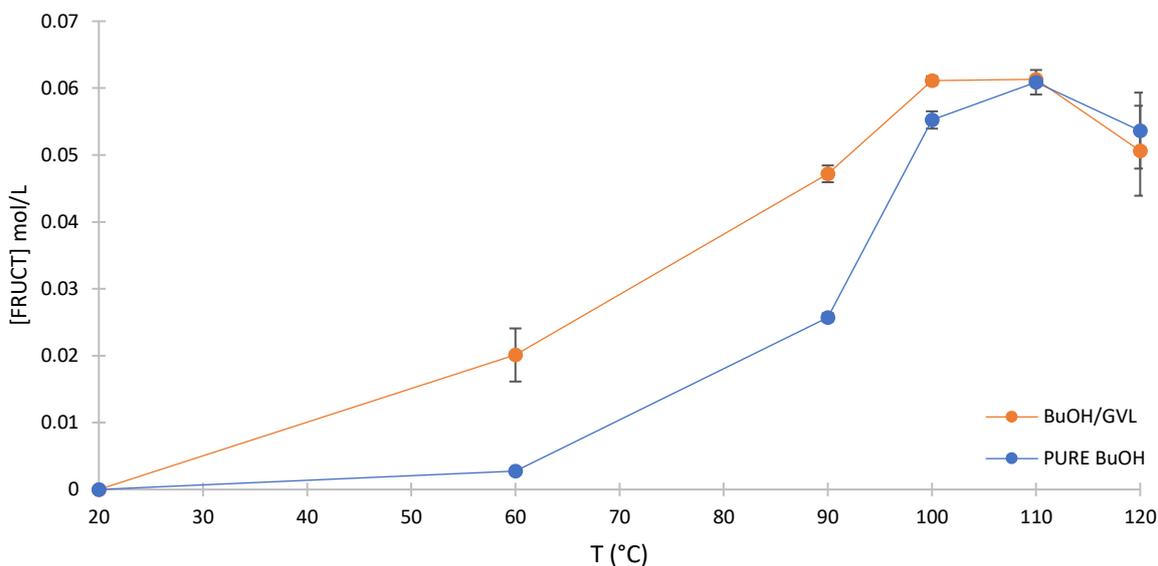

282

283   Fig. 6. Fructose dissolution in pure butanol and GVL/BuOH (30/70 wt%) solvents versus temperature.

284

285

286

287

288

289

290

291

292   3.4 Analysis of the effect of solvents in the alcoholysis of fructose.

293   -   Butanol-Water

294   From Fig. 7A, it is not possible to observe a clear trend concerning the role of water concentration on

295   the kinetics of fructose consumption since its reduction is due simultaneously to its rapid conversion to

296   HMF and degradation to humins. The trends of HMF production and consumption give a better insight

297   into the role of water. In Fig. 7B, HMF consumption is faster and total in the absence of water (Run 4,

298   Fig. 7B), whereas at the highest water concentration, 17 wt% (i.e., Run 1, Fig. 7B), its conversion is

299   slower. In high-water content, HMF is still present after 7 h, with a final yield of 18.3 %. The same water

300   effects are also reflected in BMF concentration trends (Fig. 7C). BMF shows an upward concentration

301   trend throughout the reaction time with 17 wt% of water (Run 1); by reducing the water concentration,

302   the consumption phase of this intermediate becomes more and more pronounced. From Fig. 7C, the

303   fastest kinetic is obtained in the absence of water, where the maximum of BMF is achieved at 180

304   minutes. This observation is confirmed by Fig. 7D where the BL production is faster and higher by

305   reducing the water content. The increase in BL production, i.e., in yield of BL, by decreasing the water

306   content is also directly related to the moles of fructose lost during the reaction time. Table 6 reports the

307   fructose loss (mol%) due to by-sides reactions, as degradation to humins, which amounts to around

308   22% with 17% water and is reduced to 1.5% in the absence of water, increasing BL yield of up to 57.5%.

309

310
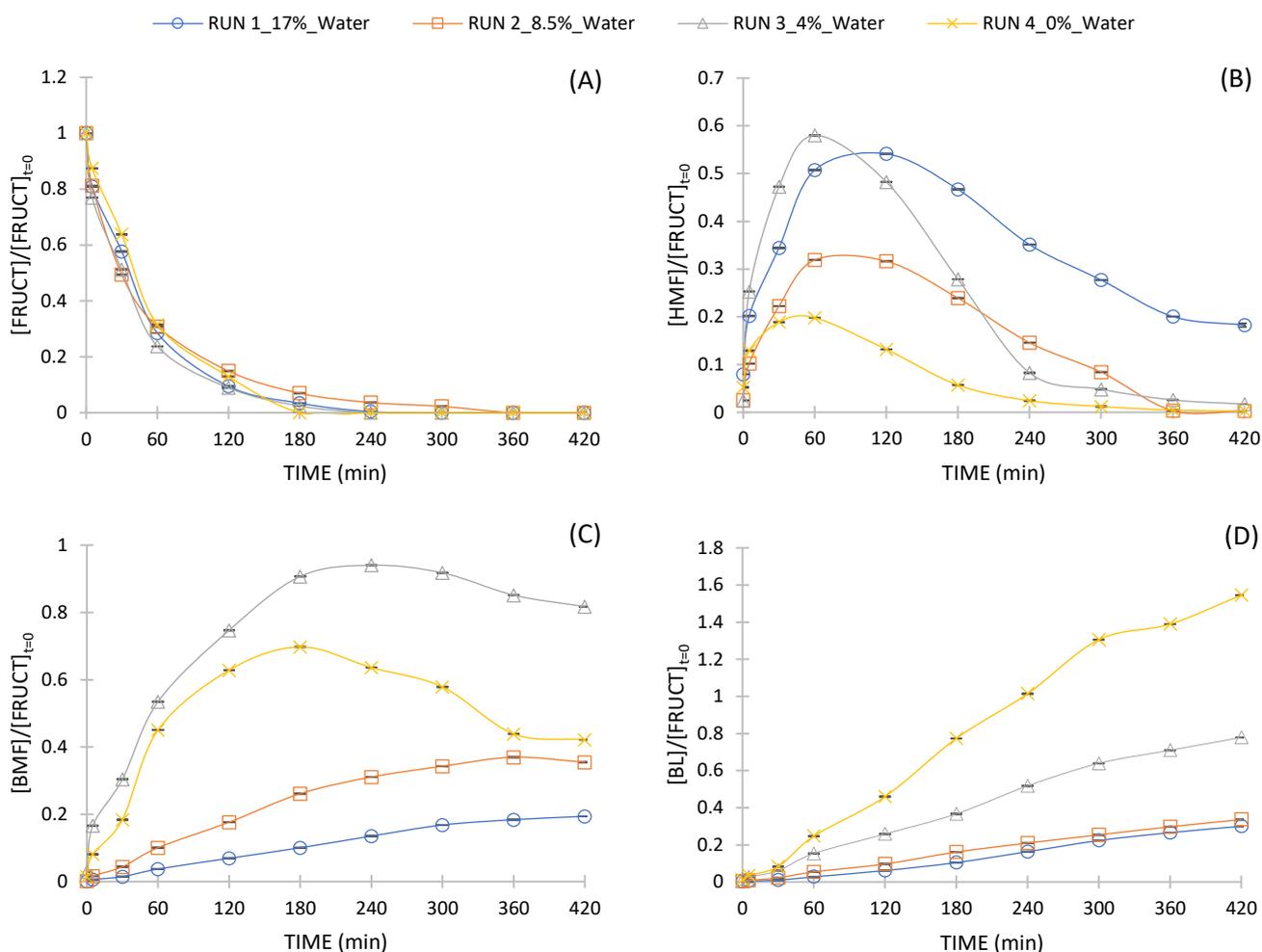
Fig. 7. Effect of water concentration on the concentrations (normalised with respect to the fructose concentration at time zero): (A) fructose, (B) HMF, (C) BMF, and (D) BL

311

312   These results may confirm the role of water in affecting the stability of fructose in alcoholic medium,

313   favoring its degradation to humins by-product [44,46,48]. Besides, to increase fructose loss into humins,

314   the role of the water in inhibiting catalytic action of ion exchange resins, as suggested by some research

315   [70,71].

316

317   Table 6: Fructose moles lost in butanol-water solvent (110 °C, fructose initial conc. 11 g/L, catalyst
318   loading 35 g/L).

Run	Butanol (wt%)	Water (wt%)	GVL (wt%)	Fructose lost mol%
1	83	17	0	22.2
2	91.5	8.5	0	16.1
3	96	4	0	5.7
4	100	0	0	1.5

319

320

321   - <u>Butanol-Water (8.5wt%)-GVL</u>

322 In these experiments, the effect of aprotic polar solvent, namely GVL, was evaluated in the solvent polar

323 protic mixture butanol-water. In this system, 8.5 wt% water was added as the minimum water content to

324 achieve the fastest fructose dissolution and thus neglect the dissolution effect on reaction kinetics.

325 Fig. 8A shows that the kinetics of fructose consumption is faster at the highest GVL concentration (i.e.,

326 Run 5). When the concentration of GVL is lower, the kinetics of fructose consumption is slower (Fig.

327 8A). This could derive from the ability of GVL to promote further the dissolution of fructose in the alcohol

328 medium, as demonstrated in the dissolution study, by facilitating the interaction with the catalyst.

329 However, the rapid fructose conversion in GVL excess is not reflected in the HMF production and

330 consumption trend, which is faster when GVL concentration decreases (Fig. 8B). This may be because

331 the reaction pathway seems to change in excess of GVL. In contrast to the other experiments, a modest

332 concentration of LA was produced in Run 5, with yields in LA of up to 15%. LA was not identified in Runs

333 5 and 6, where high concentrations of the intermediate BMF can be found. HMF concentration trends in

334 30 wt% (Run 5) and 15 wt% (Run 6) are similar, with a higher HMF concentration produced in the case

335 of 30 wt% of GVL. In both solvent systems, a residual HMF concentration can be found after 7 hours, in

336 contrast to Run 2 where a complete conversion of HMF is observed for the same water content. This

337 may highlight the role of the aprotic solvent in stabilizing reaction intermediates such as HMF. The same

338 trend was also observed for the BMF consumption and production concentration trends (Fig. 8C). From

339 Fig. 8C, the production of BMF is remarkably low at the highest GVL concentration, as a result of LA

340 production by HMF rehydration, and with an optimal production trend in 30 wt% GVL. Fig. 8D shows

341 that high GVL concentration does not increase the BL production in the reaction time considered,

342 possibly due to slower LA esterification kinetics to BL than BMF conversion and a non-excess of alcohol

343 in the medium. GVL concentration between 15 and 30 wt% gives a higher BL concentration. Low GVL

344 amount improves the production of BL compared to Run 2 in terms of yields, but a higher GVL amount

345 is detrimental for BL production (Fig. 8D). The beneficial role of GVL is also demonstrated by evaluating

346 the secondary consumption of fructose moles (Table 7), where the addition of GVL can result in up to

347 5% less of fructose lost, compared to the solvent butanol-water. As an optimum in terms of BL production

348 and fructose mole loss, experimental results indicate the addition of 30 wt% GVL in the solvent medium.

349

350 Table 7: Fructose moles lost in butanol-water-GVL solvent, compared with Run 2 (110 °C, fructose
351 initial conc. 11 g/L, catalyst loading 35 g/L).

Run	Butanol (wt%)	Water (wt%)	GVL (wt%)	Fructose lost mol%
2	91.5	8.5	0	16.1
5	2.5	8.5	89	9.1
6	60.5	8.5	30	10
7	76.5	8.5	15	11.9

352

353

354

355

356

357
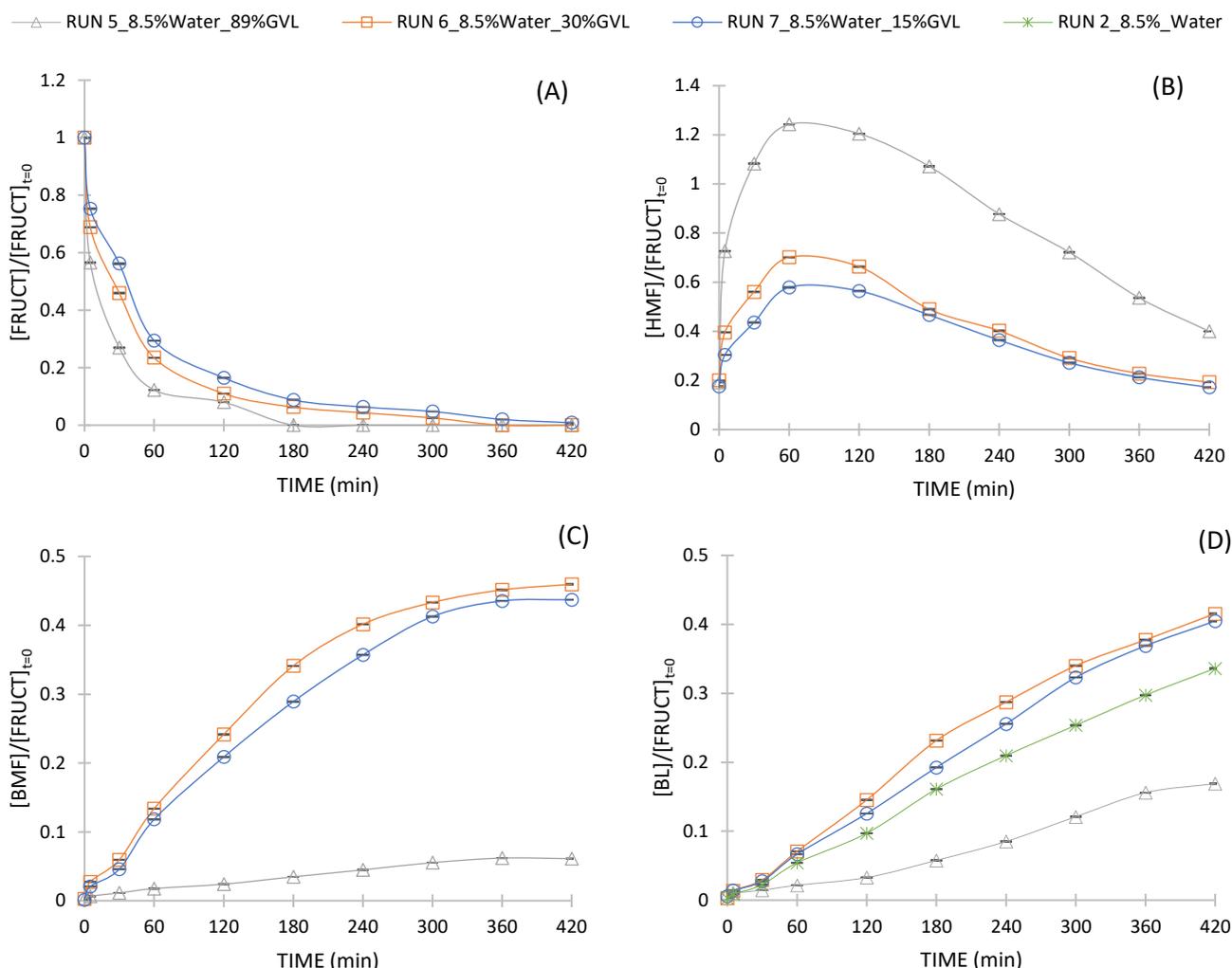
Fig. 8. Effect of GVL concentration on the concentrations (normalised with respect to the fructose concentration at time zero): (A) fructose, (B) HMF, (C) BMF, and (D) BL.

358

- Butanol-GVL in the absence of water

359

360 Previous results showed that water does not improve the fructose alcoholysis to butyl levulinate. From

361 Run 6, the addition of 30 w% of GVL increases the BL yield. A further investigation was done by

362 performing an experiment with 30 w% of GVL in the absence of water (Run 8). Fig. 9A shows that

363 fructose consumption in a 30 wt% GVL (Run 8) is slower than pure butanol. This result may be due to

364 GVL ability to limit unwanted degradation reaction to humins, resulting in higher selectivity to reaction

365 intermediates such as HMF and BMF. In fact, the production of HMF and BMF is more important at 30

366 wt% of GVL (Figs 9B and C). In 30 wt% GVL, HMF is still present in moderate concentration after 7

367 hours, whereas in pure butanol, it rapidly reaches complete conversion. As with fructose, this could be

368 due to the role of GVL in stabilising the HMF intermediate and limiting its degradation. This is also

20

369 reflected in the reduction of the moles of fructose lost, which are approximately zero in the presence of

370 GVL and greater than 1% in pure alcohol, as shown in Table 8. This observation is confirmed by Fig.

371 9D where the concentration of BL increases at 30 wt.% of BL. Although the consumption kinetics of

372 fructose and intermediates are slower in the presence of GVL, the production of BL is higher and faster

373 than in pure butanol.

374
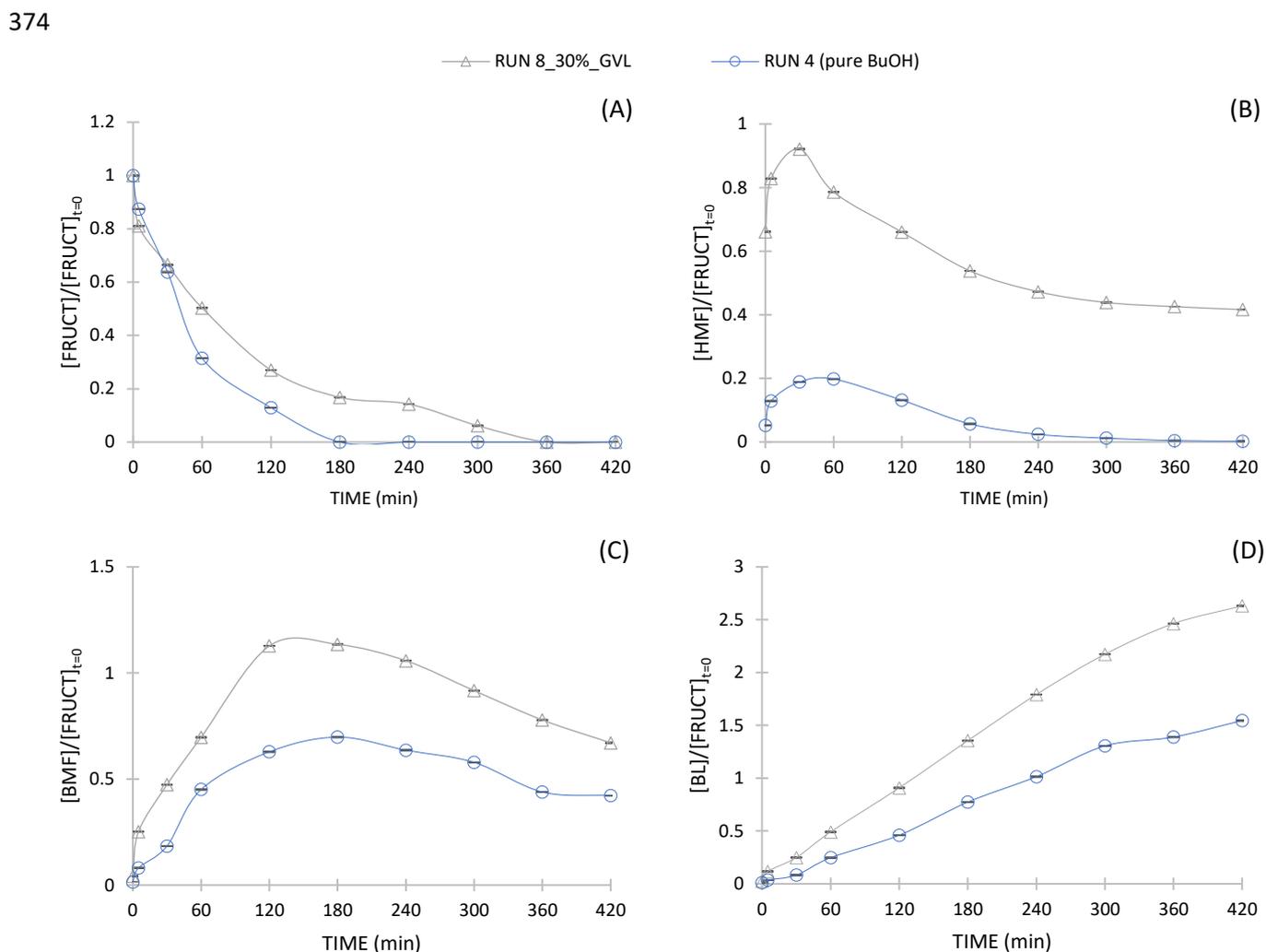
Fig. 9. Effect of BuOH/GVL concentration on the concentrations (normalised with respect to the fructose concentration at time zero): (A) fructose, (B) HMF, (C) BMF, and (D) BL.

375

376 Table 8: Comparison fructose moles lost in run 4 and 8 (110 °C, fructose initial conc. 11 g/L, catalyst
377 loading 35 g/L).

Run	Butanol wt%	Water wt%	GVL wt%	Fructose lost mol%
4	100	0	0	1.5
8	70	0	30	0

378

21

379   3.5 Comparison with literature data

380   Table 9 compared the literature data of fructose solvolysis to BL over different solid acid catalysts with

381   the most promising obtained in this study. Since other reaction conditions are used, the comparison is

382   not directly straightforward. Considering the same cross-linking grade (DVB%=8), since it directly affects

383   the catalytic activity [43], Amberlite IR120 has been compared with Amberlyst 39 and Dowex 50Wx8. In

384   the presence of water, the yield of BL obtained with Amberlite IR120 (entry 3) is slightly higher than the

385   corresponding with Dowex50Wx8 (entry 5) and Amberlyst 39 (entry 6), considering a higher catalyst

386   loading but a lower temperature and a lower acid capacity (4.4 m_{eq}/g versus 4.83 m_{eq}/g of Dowex 50Wx8

387   and 4.82 m_{eq}/g of Amberlyst 39, respectively [43]). The elimination of water from the solvent mixture

388   drastically affects the production of BL, increasing the yield to 57.5 % (entry 2) in pure butanol, from

389   30.0 % (entry 3) in the presence of 17 wt% of water. This is due to the role of water in the degradative

390   consumption of fructose leading to up to 22% of fructose moles lost, and secondly, its possible inhibiting

391   effect on the catalytic activity of the resin. As shown, the BL yield increased significantly, reaching values

392   comparable to those in the literature for other solid acid catalysts. An et al. [33] reported a 62.8 % of BL

393   yield in the presence of $Fe_2(SO_4)_3$ at 190 °C; Kuo et al. [72] obtained 67 % of BL yield by using TiO_2

394   nanoparticles at 150 °C; Balakrishnan et al. [73] found lower yields by using Dowex 50Wx8 resin, maybe

395   due to the high catalyst loading.

396   Table 9 shows that the BL production is further improved by introducing GVL in butanol solvent system

397   (30/70 wt%), leading to 60.4 % yield (entry 1). The presence of GVL also led to an increase in HMF and

398   BMF selectivity, resulting in a higher residual concentration of these intermediates after the reaction

399   time compared to the case of pure butanol. The addition of GVL determined a strong reduction in

400   fructose moles lost, up to 7% less in a solvent system with water (Table 7, run 2 versus 6), and no moles

401   lost in BuOH/GVL solvent system (table 8, run 8). The effect on fructose moles balance and the residual

402   intermediate concentrations may suggest that GVL prevents the consumption of fructose and HMF by

403   secondary reactions, such as degradation to humins, and that even higher BL yields could be expected

404   by increasing the contact time.

405   In summary, fructose alcoholysis on Amberlite IR120 achieved good BL yields, comparable to those

406   obtained in other studies but significant in energy savings under more moderate temperature conditions.

407   The use of GVL in the alcohol medium increased the butyl levulinate production and resulted in faster

408   dissolution of fructose, promising benefits from the perspective of considering production from higher

409   concentrations of fructose.

22

410   Table 9: Comparison with literature data on fructose alcoholysis to butyl levulinate.

Entry	Catalyst	T (°C)	t (h)	Fructose (g/L)	Solvent (wt%)		ω_{CAT} (g/L)	X_{fruct} %	Y_{BL} %	Ref.
1	Amberlite IR120	110	7	11	BuOH/GVL	70/30	35	100	**60.4**	This study
2		110	7	11	BuOH	-	35	100	**57.5**	
3		110	7	11	BuOH/Water	83/17	35	100	**30.0**	
4	Dowex 50Wx8	110	30	72	BuOH	-	260	97	**14.0**	[73]
5		120	6	21	BuOH/Water	83/17	14.3	>99.5	**24.2**	[43]
6	Amberlyst 39	120	6	21	BuOH/Water	83/17	14.3	>99.5	**25.3**	
7	$Fe_2(SO_4)_3$	190	3	25	BuOH	-	5	>99	**62.8**	[33]
8	TiO_2	150	1	20	BuOH	-	5	100	**67.0**	[72]
9	CNT-PSSA	120	12	12.5	BuOH	-	5	99	**78.0**	[29]

411

412

4. Conclusions

The alcoholysis of biomass-derived fructose into promising fuel additive n-butyl levulinate over ion exchange resins was studied in this research, showing the benefits of polar aprotic solvent GVL in terms of fructose dissolution and production of BL.

The swelling behavior of the catalyst was studied and found to be independent of the nature of the solvents tested. Furthermore, it has been shown that the influence of external and internal mass transfer can be neglected using 800 rpm of rotating speed and the native particle size distribution by using our experimental setup.

Among the solvent mixtures tested, BuOH/GVL (70/30 wt%) has increased fructose dissolution compared to pure butanol. Fructose dissolution was faster in BuOH/GVL (70/30 wt%) between 20 and 100°C, achieving complete dissolution at 100 °C. Temperature higher than 110 °C results in significant degradation of fructose in both solvents.

The influence of water and GVL co-solvent (polar aprotic) were investigated on the kinetics of fructose, HMF, BMF and BL. The addition of water did not improve BL production kinetics, although it promotes the rapid dissolution of fructose even at low temperatures. At the contrary, BL yield increased from 30 % with 17 wt% of water to 57.5 % in the absence of water. Finally, the yield was further increased to 60.4 % by adding 30 wt% of GVL in butanol.

Considering the fructose dissolution and kinetic results, the use of BuOH/GVL (70/30 wt%) solvent is the best solution in the alcoholysis of fructose to butyl levulinate over solid acid catalyst.

References

[1]   Valentine J, Clifton-Brown J, Hastings A, Robson P, Allison G, Smith P. Food vs. fuel: the use of land for lignocellulosic 'next generation' energy crops that minimize competition with primary food production. Global Change Biol Bioenergy 2012;4:1–19. https://doi.org/10.1111/j.1757-1707.2011.01111.x.

[2]   Wagle A, Angove MJ, Mahara A, Wagle A, Mainali B, Martins M, et al. Multi-stage pretreatment of lignocellulosic biomass for multi-product biorefinery: A review. Sustainable Energy Technologies and Assessments 2022;49:101702. https://doi.org/10.1016/j.seta.2021.101702.

[3]   Oriez V, Peydecastaing J, Pontalier P-Y. Lignocellulosic Biomass Fractionation by Mineral Acids and Resulting Extract Purification Processes: Conditions, Yields, and Purities. Molecules 2019;24:4273. https://doi.org/10.3390/molecules24234273.

[4]   Li M-F, Yang S, Sun R-C. Recent advances in alcohol and organic acid fractionation of lignocellulosic biomass. Bioresource Technology 2016;200:971–80. https://doi.org/10.1016/j.biortech.2015.10.004.

[5]   Lu X, Lagerquist L, Eränen K, Hemming J, Eklund P, Estel L, et al. Reductive Catalytic Depolymerization of Semi-industrial Wood-Based Lignin. Ind Eng Chem Res 2021;60:16827–38. https://doi.org/10.1021/acs.iecr.1c03154.

[6]   Ragauskas AJ, Beckham GT, Biddy MJ, Chandra R, Chen F, Davis MF, et al. Lignin Valorization: Improving Lignin Processing in the Biorefinery. Science 2014;344:1246843. https://doi.org/10.1126/science.1246843.

[7]   Rinaldi R, Jastrzebski R, Clough MT, Ralph J, Kennema M, Bruijnincx PCA, et al. Paving the Way for Lignin Valorisation: Recent Advances in Bioengineering, Biorefining and Catalysis. Angew Chem Int Ed 2016;55:8164–215. https://doi.org/10.1002/anie.201510351.

[8]   Sun Z, Fridrich B, de Santi A, Elangovan S, Barta K. Bright Side of Lignin Depolymerization: Toward New Platform Chemicals. Chem Rev 2018;118:614–78. https://doi.org/10.1021/acs.chemrev.7b00588.

473 [9] Azadi P, Inderwildi OR, Farnood R, King DA. Liquid fuels, hydrogen and chemicals from lignin:

474 A critical review. Renewable and Sustainable Energy Reviews 2013;21:506–23.

475 https://doi.org/10.1016/j.rser.2012.12.022.

476 [10] Liu C, Wu S, Zhang H, Xiao R. Catalytic oxidation of lignin to valuable biomass-based platform

477 chemicals: A review. Fuel Processing Technology 2019;191:181–201.

478 https://doi.org/10.1016/j.fuproc.2019.04.007.

479 [11] Zhou M, Sharma BK, Li J, Zhao J, Xu J, Jiang J. Catalytic valorization of lignin to liquid fuels over

480 solid acid catalyst assisted by microwave heating. Fuel 2019;239:239–44.

481 https://doi.org/10.1016/j.fuel.2018.10.144.

482 [12] Kumar AK, Sharma S. Recent updates on different methods of pretreatment of lignocellulosic

483 feedstocks: a review. Bioresour Bioprocess 2017;4:7. https://doi.org/10.1186/s40643-017-0137-9.

484 [13] Zhang Z, Song J, Han B. Catalytic Transformation of Lignocellulose into Chemicals and Fuel

485 Products in Ionic Liquids. Chem Rev 2017;117:6834–80.

486 https://doi.org/10.1021/acs.chemrev.6b00457.

487 [14] Loow Y-L, Wu TY, Md. Jahim J, Mohammad AW, Teoh WH. Typical conversion of lignocellulosic

488 biomass into reducing sugars using dilute acid hydrolysis and alkaline pretreatment. Cellulose

489 2016;23:1491–520. https://doi.org/10.1007/s10570-016-0936-8.

490 [15] Luo Y, Li Z, Li X, Liu X, Fan J, Clark JH, et al. The production of furfural directly from hemicellulose

491 in lignocellulosic biomass: A review. Catalysis Today 2019;319:14–24.

492 https://doi.org/10.1016/j.cattod.2018.06.042.

493 [16] Rajesh Banu J, Preethi, Kavitha S, Tyagi VK, Gunasekaran M, Karthikeyan OP, et al.

494 Lignocellulosic biomass based biorefinery: A successful platform towards circular bioeconomy. Fuel

495 2021;302:121086. https://doi.org/10.1016/j.fuel.2021.121086.

496 [17] Reshmy R, Paulose TAP, Philip E, Thomas D, Madhavan A, Sirohi R, et al. Updates on high value

497 products from cellulosic biorefinery. Fuel 2022;308:122056.

498 https://doi.org/10.1016/j.fuel.2021.122056.

499 [18] Cherubini F, Strømman AH. Production of Biofuels and Biochemicals from Lignocellulosic

500 Biomass: Estimation of Maximum Theoretical Yields and Efficiencies Using Matrix Algebra. Energy Fuels

501 2010;24:2657–66. https://doi.org/10.1021/ef901379s.

502 [19] Isikgor FH, Becer CR. Lignocellulosic biomass: a sustainable platform for the production of bio-

503 based chemicals and polymers. Polymer Chemistry 2015;6:4497–559.

504 https://doi.org/10.1039/C5PY00263J.

505 [20] Badgujar KC, Badgujar VC, Bhanage BM. A review on catalytic synthesis of energy rich fuel

506 additive levulinate compounds from biomass derived levulinic acid. Fuel Processing Technology

507 2020;197:106213. https://doi.org/10.1016/J.FUPROC.2019.106213.

508 [21] Kothe V, Melfi DT, dos Santos KC, Corazza ML, Ramos LP. Thermodynamic analysis,

509 experimental and kinetic modeling of levulinic acid esterification with ethanol at supercritical

510 conditions. Fuel 2020;260:116376. https://doi.org/10.1016/j.fuel.2019.116376.

511 [22] Vilanculo CB, de Andrade Leles LC, da Silva MJ. H4SiW12O40-Catalyzed Levulinic Acid

512 Esterification at Room Temperature for Production of Fuel Bioadditives. Waste and Biomass

513 Valorization 2020;11:1895–904. https://doi.org/10.1007/s12649-018-00549-x.

514 [23] Badia JH, Ramírez E, Soto R, Bringué R, Tejero J, Cunill F. Optimization and green metrics

515 analysis of the liquid-phase synthesis of sec-butyl levulinate by esterification of levulinic acid with 1-

516 butene over ion-exchange resins. Fuel Processing Technology 2021;220:106893.

517 https://doi.org/10.1016/j.fuproc.2021.106893.

518 [24] Liu C, Lu X, Yu Z, Xiong J, Bai H, Zhang R. Production of Levulinic Acid from Cellulose and

519 Cellulosic Biomass in Different Catalytic Systems. Catalysts 2020;10:1006.

520 https://doi.org/10.3390/catal10091006.

521 [25] Signoretto M, Taghavi S, Ghedini E, Menegazzo F. Catalytic Production of Levulinic Acid (LA)

522 from Actual Biomass. Molecules 2019;24:2760. https://doi.org/10.3390/molecules24152760.

523 [26] Al Shaal MG. Transformation of Levulinic Acid and Intermediates Thereof into Potential Biofuel

524 Compounds over Heterogeneous Catalysts. RWTH Aachen University, 2016.

525 [27] Alonso DM, Wettstein SG, Dumesic JA. Gamma-valerolactone, a sustainable platform molecule

526 derived from lignocellulosic biomass. Green Chem 2013;15:584. https://doi.org/10.1039/c3gc37065h.

527 [28] van Zandvoort I, Wang Y, Rasrendra CB, van Eck ERH, Bruijnincx PCA, Heeres HJ, et al.

528 Formation, Molecular Structure, and Morphology of Humins in Biomass Conversion: Influence of

529 Feedstock and Processing Conditions. ChemSusChem 2013;6:1745–58.

530 https://doi.org/10.1002/cssc.201300332.

531 [29] Liu R, Chen J, Huang X, Chen L, Ma L, Li X. Conversion of fructose into 5-hydroxymethylfurfural

532 and alkyl levulinates catalyzed by sulfonic acid-functionalized carbon materials. Green Chem

533 2013;15:2895. https://doi.org/10.1039/c3gc41139g.

534 [30] Yu X, Peng L, Dai J, Li H, Tao C, Yang F, et al. Ethylene glycol co-solvent enhances alkyl levulinate

535 production from concentrated feeds of sugars in monohydric alcohols. Fuel 2021;304:121471.

536 https://doi.org/10.1016/j.fuel.2021.121471.

537 [31] Chang C, Xu G, Zhu W, Bai J, Fang S. One-pot production of a liquid biofuel candidate—Ethyl

538 levulinate from glucose and furfural residues using a combination of extremely low sulfuric acid and

539 zeolite USY. Fuel 2015;140:365–70. https://doi.org/10.1016/j.fuel.2014.09.102.

540 [32] Peng L, Lin L, Zhang J, Shi J, Liu S. Solid acid catalyzed glucose conversion to ethyl levulinate.

541 Applied Catalysis A: General 2011;397:259–65. https://doi.org/10.1016/j.apcata.2011.03.008.

542 [33] An R, Xu G, Chang C, Bai J, Fang S. Efficient one-pot synthesis of n-butyl levulinate from

543 carbohydrates catalyzed by Fe2(SO4)3. Journal of Energy Chemistry 2017;26:556–63.

544 https://doi.org/10.1016/J.JECHEM.2016.11.015.

545 [34] Peng L, Gao X, Chen K. Catalytic upgrading of renewable furfuryl alcohol to alkyl levulinates

546 using AlCl3 as a facile, efficient, and reusable catalyst. Fuel 2015;160:123–31.

547 https://doi.org/10.1016/J.FUEL.2015.07.086.

548 [35] Peixoto AF, Ramos R, Moreira MM, Soares OSGP, Ribeiro LS, Pereira MFR, et al. Production of

549 ethyl levulinate fuel bioadditive from 5-hydroxymethylfurfural over sulfonic acid functionalized

550 biochar catalysts. Fuel 2021;303:121227. https://doi.org/10.1016/J.FUEL.2021.121227.

551   [36]   Windom BC, Lovestead TM, Mascal M, Nikitin EB, Bruno TJ. Advanced Distillation Curve

552   Analysis on Ethyl Levulinate as a Diesel Fuel Oxygenate and a Hybrid Biodiesel Fuel. Energy and Fuels

553   2011;25:1878–90. https://doi.org/10.1021/EF200239X.

554   [37]   Joshi H, Moser BR, Toler J, Smith WF, Walker T. Ethyl levulinate: A potential bio-based diluent

555   for biodiesel which improves cold flow properties. Biomass and Bioenergy 2011;35:3262–6.

556   https://doi.org/10.1016/J.BIOMBIOE.2011.04.020.

557   [38]   Tian M, McCormick RL, Luecke J, de Jong E, van der Waal JC, van Klink GPM, et al. Anti-knock

558   quality of sugar derived levulinic esters and cyclic ethers. Fuel 2017;202:414–25.

559   https://doi.org/10.1016/J.FUEL.2017.04.027.

560   [39]   Wang Z, Lei T, Lin L, Yang M, Li Z, Xin X, et al. Comparison of the Physical and Chemical

561   Properties, Performance, and Emissions of Ethyl Levulinate–Biodiesel–Diesel and *n* -Butanol–

562   Biodiesel–Diesel   Blends.   Energy   Fuels   2017;31:5055–62.

563   https://doi.org/10.1021/acs.energyfuels.6b02851.

564   [40]   Christensen E, Williams A, Paul S, Burton S, McCormick RL. Properties and Performance of

565   Levulinate Esters as Diesel Blend Components. Energy and Fuels 2011;25:5422–8.

566   https://doi.org/10.1021/EF201229J.

567   [41]   Frigo S, Pasini G, Caposciutti G, Antonelli M, Galletti AMR, Gori S, et al. Utilisation of advanced

568   biofuel in CI internal combustion engine. Fuel 2021;297:120742.

569   https://doi.org/10.1016/J.FUEL.2021.120742.

570   [42]   Di Menno Di Bucchianico D, Wang Y, Buvat J-C, Pan Y, Casson Moreno VC, Leveneur S.

571   Production of levulinic acid and alkyl levulinates: A process insight. Green Chem 2021.

572   https://doi.org/10.1039/D1GC02457D.

573   [43]   Ramírez E, Bringué R, Fité C, Iborra M, Tejero J, Cunill F. Assessment of ion exchange resins as

574   catalysts for the direct transformation of fructose into butyl levulinate. Applied Catalysis A: General

575   2021;612:117988. https://doi.org/10.1016/J.APCATA.2021.117988.

576 [44] Sun Y, Sun K, Zhang L, Zhang S, Liu Q, Wang Y, et al. Impacts of Solvents on the Stability of the

577 Biomass-Derived Sugars and Furans. Energy Fuels 2020;34:3250–61.

578 https://doi.org/10.1021/acs.energyfuels.9b03921.

579 [45] Bagno A, Scorrano G. Selectivity in Proton Transfer, Hydrogen Bonding, and Solvation. Acc

580 Chem Res 2000;33:609–16. https://doi.org/10.1021/ar990149j.

581 [46] Guo H, Duereh A, Su Y, Hensen EJM, Qi X, Smith RL. Mechanistic role of protonated polar

582 additives in ethanol for selective transformation of biomass-related compounds. Applied Catalysis B:

583 Environmental 2020;264:118509. https://doi.org/10.1016/j.apcatb.2019.118509.

584 [47] Guo H, Qi X, Hiraga Y, Aida TM, Smith RL. Efficient conversion of fructose into 5-

585 ethoxymethylfurfural with hydrogen sulfate ionic liquids as co-solvent and catalyst. Chemical

586 Engineering Journal 2017;314:508–14. https://doi.org/10.1016/j.cej.2016.12.008.

587 [48] Karnjanakom S, Maneechakr P, Samart C, Guan G. A facile way for sugar transformation

588 catalyzed by carbon-based Lewis-Brønsted solid acid. Molecular Catalysis 2019;479:110632.

589 https://doi.org/10.1016/j.mcat.2019.110632.

590 [49] Raspolli Galletti AM, Antonetti C, Fulignati S, Licursi D. Direct Alcoholysis of Carbohydrate

591 Precursors and Real Cellulosic Biomasses to Alkyl Levulinates: A Critical Review. Catalysts

592 2020;10:1221. https://doi.org/10.3390/catal10101221.

593 [50] Iborra M, Tejero J, Fité C, Ramírez E, Cunill F. Liquid-phase synthesis of butyl levulinate with

594 simultaneous water removal catalyzed by acid ion exchange resins. Journal of Industrial and

595 Engineering Chemistry 2019;78:222–31. https://doi.org/10.1016/j.jiec.2019.06.011.

596 [51] Covinich LG, Clauser NM, Felissia FE, Vallejos ME, Area MC. The challenge of converting

597 biomass polysaccharides into levulinic acid through heterogeneous catalytic processes. Biofuels,

598 Bioprod Bioref 2020;14:417–45. https://doi.org/10.1002/bbb.2062.

599 [52] Mellmer MA, Sener C, Gallo JMR, Luterbacher JS, Alonso DM, Dumesic JA. Solvent Effects in

600 Acid-Catalyzed Biomass Conversion Reactions. Angew Chem Int Ed 2014;53:11872–5.

601 https://doi.org/10.1002/anie.201408359.

602 [53]   Wang Y, Cipolletta M, Vernières-Hassimi L, Casson-Moreno V, Leveneur S. Application of the

603   concept of Linear Free Energy Relationships to the hydrogenation of levulinic acid and its

604   corresponding   esters.   Chemical   Engineering   Journal   2019;374:822–31.

605   https://doi.org/10.1016/j.cej.2019.05.218.

606 [54]   Capecci S, Wang Y, Delgado J, Casson Moreno V, Mignot M, Grénman H, et al. Bayesian

607   Statistics to Elucidate the Kinetics of γ-Valerolactone from n-Butyl Levulinate Hydrogenation over

608   Ru/C. Ind Eng Chem Res 2021;31:11725–36. https://doi.org/10.1021/acs.iecr.1c02107.

609 [55]   Kerkel F, Markiewicz M, Stolte S, Müller E, Kunz W. The green platform molecule gamma-

610   valerolactone – ecotoxicity, biodegradability, solvent properties, and potential applications. Green

611   Chem 2021;23:2962–76. https://doi.org/10.1039/D0GC04353B.

612 [56]   Anastas PT, Warner JC. Green Chemistry: Theory and Practice. Oxford University Press: New

613   York; 1998.

614 [57]   Srinivas G, Unny VKP, Mukkanti K, Choudary BM. A convenient photosynthesis of uniformly

615   [14C]-labelled d-glucose, d-fructose and sucrose, and chemical synthesis of methyl-α-d-

616   glucopyranoside   ([U-14C]-glucose).   Applied   Radiation   and   Isotopes   2013;72:145–51.

617   https://doi.org/10.1016/j.apradiso.2012.10.016.

618 [58]   Russo V, Tesser R, Rossano C, Cogliano T, Vitiello R, Leveneur S, et al. Kinetic study of Amberlite

619   IR120 catalyzed acid esterification of levulinic acid with ethanol: From batch to continuous operation.

620   Chemical Engineering Journal 2020;401:126126. https://doi.org/10.1016/J.CEJ.2020.126126.

621 [59]   Altıokka MR, Çıtak A. Kinetics study of esterification of acetic acid with isobutanol in the

622   presence   of   amberlite   catalyst.   Applied   Catalysis   A: General   2003;239:141–8.

623   https://doi.org/10.1016/S0926-860X(02)00381-2.

624 [60]   Jogunola O, Salmi T, Eränen K, Mikkola J-P. Qualitative treatment of catalytic hydrolysis of alkyl

625   formates.   Applied   Catalysis   A: General   2010;384:36–44.

626   https://doi.org/10.1016/j.apcata.2010.06.002.

627   [61]   Mukesh C, Nikjoo D, Mikkola J-P. Production of C-14 Levulinate Ester from Glucose

628   Fermentation Liquors Catalyzed by Acidic Ionic Liquids in a Solvent-Free Self-Biphasic System. ACS

629   Omega 2020;5:4828–35. https://doi.org/10.1021/acsomega.9b03517.

630   [62]   Leveneur S, Murzin DYu, Salmi T, Mikkola J-P, Kumar N, Eränen K, et al. Synthesis of

631   peroxypropionic acid from propionic acid and hydrogen peroxide over heterogeneous catalysts.

632   Chemical Engineering Journal 2009;147:323–9. https://doi.org/10.1016/j.cej.2008.11.045.

633   [63]   Bodamer GW, Kunin R. Behavior of Ion Exchange Resins in Solvents Other Than Water -

634   Swelling and Exchange Characteristics. Industrial & Engineering Chemistry 2002;45:2577–80.

635   https://doi.org/10.1021/IE50527A057.

636   [64]   Bodamer GW, Kunin R. Behavior of Ion Exchange Resins in Solvents Other Than Water -

637   Swelling   and   Exchange   Characteristics.   Ind   Eng   Chem   1953;45:2577–80.

638   https://doi.org/10.1021/ie50527a057.

639   [65]   Königsberger E. Guidelines for the Measurement of Solid–Liquid Solubility. Journal of Chemical

640   & Engineering Data n.d.;64:381–5. https://doi.org/10.1021/acs.jced.8b01263.

641   [66]   Engasser J-M, Chamouleau F, Chebil L, Ghoul M. Kinetic modeling of glucose and fructose

642   dissolution   in   2-methyl   2-butanol.   Biochemical   Engineering   Journal   2008;42:159–65.

643   https://doi.org/10.1016/j.bej.2008.06.013.

644   [67]   Flannelly T, Dooley S, Leahy JJ. Reaction Pathway Analysis of Ethyl Levulinate and 5-

645   Ethoxymethylfurfural from D-Fructose Acid Hydrolysis in Ethanol. Energy Fuels 2015;29:7554–65.

646   https://doi.org/10.1021/acs.energyfuels.5b01481.

647   [68]   Démolis A, Essayem N, Rataboul F. Synthesis and Applications of Alkyl Levulinates. ACS

648   Sustainable Chem Eng 2014;2:1338–52. https://doi.org/10.1021/sc500082n.

649   [69]   Ahmad E, Alam MdI, Pant KK, Haider MA. Catalytic and mechanistic insights into the production

650   of   ethyl   levulinate   from   biorenewable   feedstocks.   Green   Chem   2016;18:4804–23.

651   https://doi.org/10.1039/C6GC01523A.

652 [70] du Toit E, Nicol W. The rate inhibiting effect of water as a product on reactions catalysed by

653 cation exchange resins: formation of mesityl oxide from acetone as case study. Applied Catalysis A:

654 General 2004;277:219–25. https://doi.org/10.1016/j.apcata.2004.09.015.

655 [71] Pérez MA, Bringué R, Iborra M, Tejero J, Cunill F. Ion exchange resins as catalysts for the liquid-

656 phase dehydration of 1-butanol to di-n-butyl ether. Applied Catalysis A: General 2014;482:38–48.

657 https://doi.org/10.1016/j.apcata.2014.05.017.

658 [72] Kuo CH, Poyraz AS, Jin L, Meng Y, Pahalagedara L, Chen SY, et al. Heterogeneous acidic TiO2

659 nanoparticles for efficient conversion of biomass derived carbohydrates. Green Chem 2014:785–91.

660 https://doi.org/10.1039/C3GC40909K.

661 [73] Balakrishnan M, Sacia ER, Bell AT. Etherification and reductive etherification of 5-

662 (hydroxymethyl)furfural: 5-(alkoxymethyl)furfurals and 2,5-bis(alkoxymethyl)furans as potential bio-

663 diesel candidates. Green Chem 2012;14:1626. https://doi.org/10.1039/c2gc35102a.

664

665